



You have downloaded a document from
RE-BUŚ
repository of the University of Silesia in Katowice

Title: Physicochemical analysis of Bi₂Te₃ - (Fe, Eu) - Bi₂Te₃ junctions grown by molecular beam epitaxy method

Author: Katarzyna Balin, Rafał Rapacz, Mateusz Weis, Jacek Szade

Citation style: Balin Katarzyna, Rapacz Rafał, Weis Mateusz, Szade Jacek. (2017). Physicochemical analysis of Bi₂Te₃ - (Fe, Eu) - Bi₂Te₃ junctions grown by molecular beam epitaxy method. "AIP Advances" (Vol. 7, iss. 5 (2017), art. no. 056323, s. 1-6), doi 10.1063/1.4978005



Uznanie autorstwa - Licencja ta pozwala na kopiowanie, zmienianie, rozprowadzanie, przedstawianie i wykonywanie utworu jedynie pod warunkiem oznaczenia autorstwa.



UNIwersYTET ŚLĄSKI
W KATOWICACH



Biblioteka
Uniwersytetu Śląskiego



Ministerstwo Nauki
i Szkolnictwa Wyższego

Physicochemical analysis of Bi_2Te_3 – (Fe, Eu) – Bi_2Te_3 junctions grown by molecular beam epitaxy method

K. Balin,^{1,2} R. Rapacz,^{1,2} M. Weis,^{1,2} and J. Szade^{1,2}

¹Silesian Center for Education and Interdisciplinary Research, University of Silesia, 75 Pułku Piechoty 1A, 41-500 Chorzów, Poland

²A. Chełkowski Institute of Physics, University of Silesia, Uniwersytecka 14, 40-007 Katowice, Poland

(Presented 2 November 2016; received 23 September 2016; accepted 29 November 2016; published online 2 March 2017)

Topological insulators (TI) are a class of materials gaining in importance due to their unique spin/electronic properties, which may allow for the generation of quasiparticles and electronic states which are not accessible in classical condensed-matter systems. Not surprisingly, TI are considered as promising materials for multiple applications in next generation electronic or spintronic devices, as well as for applications in energy conversion, such as thermo-electrics. In this study, we examined the practical challenges associated with the formation of a well-defined junction between a model 3D topological insulator, Bi_2Te_3 , and a metal, Fe or Eu, from which spin injection could potentially be realized. The properties of multilayer systems grown by molecular beam epitaxy (MBE), with Fe or Eu thin films sandwiched between two Bi_2Te_3 layers, were studied *in-situ* using electron diffraction and photoelectron spectroscopy. Their magnetic properties were measured using a SQUID magnetometer, while the in-depth chemical structure was assessed using secondary ion mass spectroscopy. An examination of impact of Bi_2Te_3 structure on chemical stability of the junction area has been realized. For Fe, we found that despite room temperature growth, a reaction between the Fe film and Bi_2Te_3 takes place, leading to the formation of FeTe and also the precipitation of metallic Bi. For the Eu tri-layer, a reaction also occurs, but the Te chemical state remains intact. © 2017 Author(s). All article content, except where otherwise noted, is licensed under a Creative Commons Attribution (CC BY) license (<http://creativecommons.org/licenses/by/4.0/>). [<http://dx.doi.org/10.1063/1.4978005>]

I. INTRODUCTION

Topological Insulators (TI) are a new quantum state of matter which exhibits unique quantum-mechanical properties, driving peculiar characteristics of the surface states.^{1,2} It is well known that defects, strain and doping influence the existence of metallic surface states. The explanations of particular effects observed in pure TI are complex, and become even more complicated when TI heterostructures are considered. In such cases, quantum proximity effects must be considered, but one also must inevitably consider the effects of inter-diffusion and chemical stability as well. Although studies of phenomena occurring at the interfaces of TI heterostructures were recently conducted, knowledge in this field is in its infancy. The effects related to TI - metal interfaces are very important from both a fundamental and application point of view. Due to their exotic spin nature and topological protection of the surface states, TI are viewed as promising materials for multiple applications in next generation electronic or spintronic devices. There are many ideas for novel TI-based devices,^{3,4} which would use the surface electronic states, and would allow for spin manipulation via ferromagnetic electrodes. Such devices could be based on TI – ferromagnetic (FM) junctions, in concept made to inject spins from the ferromagnetic contact to the TI material. Spin transport properties across FM/TI interfaces have been studied by ferromagnetic resonance (FMR).⁵⁻⁷ The engineering of such junctions is a crucial step for further development of diverse TI-based spintronic devices. Unfortunately, reports on the fabrication of such devices have been rare, which is inevitably connected to the technical

challenges of their engineering. To help overcome these engineering issues, our main point of interest is directed towards obtaining a detailed and broad characterization of TI-metal heterostructures. Such characterization includes analysis of crystallographic, electronic, and chemical structure, but is also aimed at the determination of their transport and magnetic properties.

II. EXPERIMENTAL DETAILS

For our model TI, we have chosen bismuth telluride; a material with well-known electronic structure, good separation of the core levels of heterostructure components (XPS spectra), and a number of high quality papers describing its properties.⁸⁻¹⁰ For the fabrication of heterostructures with Bi₂Te₃ TI, we selected two magnetic metals (M) which are potential electrodes for the future devices. One of those metals, Fe, is a well-known ferromagnet with relatively stable ferromagnetic properties starting from several monolayers.¹¹ We also selected one of the rare earth metals, Eu, mostly due to the fact that rare earths have a localized magnetic moment connected with the partly filled *4f* shells. Divalent Europium exhibits a high, pure spin magnetic moment, but its valence is unstable, and trivalent europium is non-magnetic.¹²

The subjects of our analysis are heterostructures prepared in the form of a multilayer stack of alternately deposited Bi₂Te₃ and (*3d*, *4f*)-M layers on a mica substrate. Monocrystalline mica was selected to allow for monocrystalline growth of the Bi₂Te₃ film. A Molecular Beam Epitaxy (MBE) system was used to grow each layer of the heterostructures, starting from growth in co-deposition mode of the 15nm thick, monocrystalline Bi₂Te₃ film. The next step was to deposit the M layer of ~2 nm thick iron or europium, and then finally to cap the structure with an additional 2 nm thick Bi₂Te₃ layer. Figure 1a is a visual representation of the final structure. For us, the regions of interest were located at both of the TI – (*3d*, *4f*)-M interfaces. Since Bi₂Te₃ grows in a quintuple layer (QL ~ 1 nm) structure with the lattice parameters $a=4.38 \text{ \AA}$, $c=30.49 \text{ \AA}$ we decided to focus on two cases; (1) interfacing 15 QLs of Bi₂Te₃ with the Fe or Eu, (2) interfacing the Fe or Eu layer with 2 QLs of Bi₂Te₃.

The *in-situ* measurements were made at each step of the deposition process, while the *ex-situ* measurements were performed after the growth of the entire heterostructure. Our studies were predominantly done in a large ultra-high vacuum (UHV) cluster, which connects the growth chamber with the analytical chamber under UHV conditions, allowing for *in-situ* crystallographic characterization (Reflection High Energy Electron Diffraction, Low Energy Electron Diffraction) and electronic structure determination (X-ray Photoelectron Spectroscopy). Certain magnetic and chemical properties of these heterostructures were then determined *ex-situ* using a SQUID magnetometer, while a 3D analysis of the chemical structure was performed using Time of Flight Secondary Ion Mass Spectrometry (TOF-SIMS).

III. RESULTS AND DISCUSSIONS

The crystallographic measurements, RHEED and LEED, indicated growth of monocrystalline iron (see Fig. 1c), polycrystalline europium (see Fig. 1f), on the surface of monocrystalline 15 nm thick Bi₂Te₃ (Fig. 1d and 1g). Visible at the RHEED diffraction pattern of europium weak streaks (see Fig 1f) are associated with the underlying Bi₂Te₃ layer. The top Bi₂Te₃ layer deposited on iron exhibits monocrystalline structure (see Fig. 1b), whereas the Bi₂Te₃ deposited on the europium layer is polycrystalline (see Fig 1e). LEED measurements show that the monocrystalline Bi₂Te₃ layers crystallize in a trigonal system. Weak LEED pattern have been observed for Fe deposited on 15 nm thick Bi₂Te₃ layer (see Fig 1c round shaped inset). Additional layers of Eu or TI do not give a LEED diffraction pattern, indicating the lack of single-crystalline structure.

Angle dependent XPS measurements were performed to determine the electronic structure at the interfaces. Two different analysis geometries were used to change the surface sensitivity of the measurements (studies performed with tilted heterostructures). Particular attention was paid to the chemical states at the TI-(*3d*, *4f*)-M junction, done mostly by detecting evidence of a chemical reaction between junction components. In previous work, we precisely studied the electronic and crystalline structure of non-stoichiometric polycrystalline Bi_xTe_y thin films¹³ as well as stoichiometric Bi₂Te₃

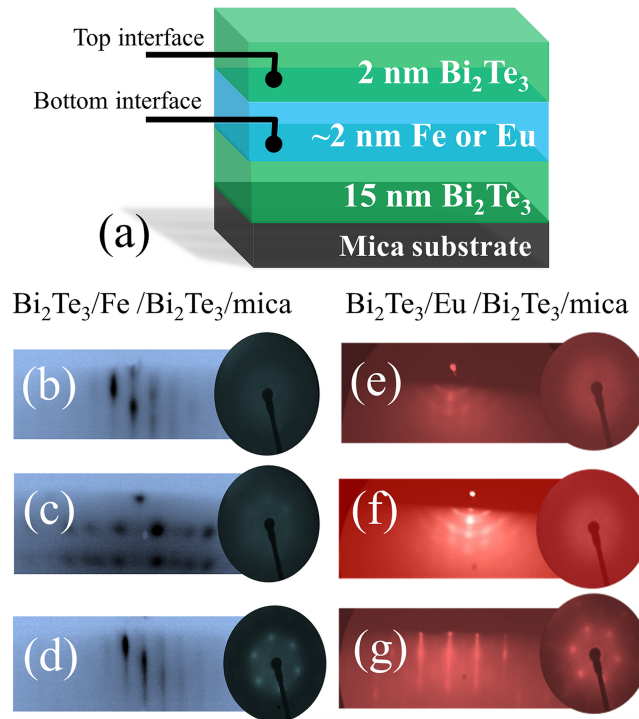


FIG. 1. Structure of deposited heterostructures (a) combined with diffraction patterns obtained with the use of RHEED and LEED at each step of deposition process for (b) 2nm of Bi_2Te_3 top layer, (c) 2.4nm Fe, (d) 15nm Bi_2Te_3 bottom layer along [100] direction, (e) 2nm Bi_2Te_3 top layer, (c) 2 nm Eu, (d) 15nm of Bi_2Te_3 bottom layer along [1-20] direction.

monocrystalline films.¹⁴ Based on that knowledge, we are able to distinguish effects related to the widely understood disorder from effects occurring due to interfacing the TI surface with the surface of deposited on TI layer metal.

The results of XPS measurements (see Fig 2) allowed us to analyze the behavior of the sample in several different aspects. First, Eu remains in the divalent state (see Fig. 2(a1)–2(a3)), however some weak $\text{Eu}^{2+} \leftrightarrow \text{Eu}^{3+}$ transition were observed in measurements of the bottom Eu- Bi_2Te_3 interface (highlighted yellow area and Fig. 2(a2)). A weak $\text{Eu}^{2+} \leftrightarrow \text{Eu}^{3+}$ transition was observed for

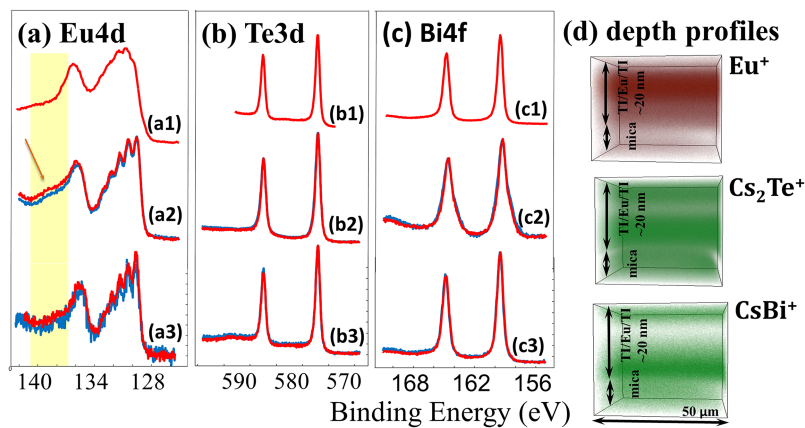


FIG. 2. The XPS photoemission spectra of (a) Eu4d (b) Te3d (c) Bi4f. Spectra obtained (a1) for 20nm thick Eu grown on Mo substrate, (b1, c1) Te3d and Bi4f of 15 nm thick Bi_2Te_3 layer respectively, (a2, b2, c2) after deposition of 2 nm thick Eu layer, (a3, b3, c3) after deposition of 2 nm thick Bi_2Te_3 top layer. Blue lines correspond to angle dependent XPS measurements. 3D depth profiles (d) represent distribution of Eu ions and (Te or Bi) cesium ions within the heterostructure.

heterostructures with 2 nm thick Eu, while for the heterostructure with 0.5 nm thick Eu (not shown), this transition was not observed. For Eu in the divalent state, exchange splitting leads to the very well resolved structure of the Eu $4d_{5/2}$ core level seen in Fig. 2(a2–3). The splitting of particular states, which can be ascribed to the various 9D_J final states, is measured to be 0.9 eV, the same as in pure Eu. Interestingly, the known effect of reduced intensity of the lowest binding energy lines originating from the high spin states¹⁵ (see referenced spectrum of pure europium Fig. 2(a1)) is, surprisingly, removed by when Eu is in contact with Bi_2Te_3 (Fig. 2(a2) and 2(a3)). This phenomenon requires further studies. Inter-mixing of the junction components at room temperature was observed, the evidence of which was seen in the chemical shifts of the core levels, as well as in the TOF-SIMS depth profiles. The influence of the Eu layer on the electronic structure of the bottom Bi_2Te_3 layer manifests in the $\text{Bi}4f$ spectrum as an additional chemical state of Bi (see Fig. 2(c2)), clearly visible as a broadening of the $\text{Bi}4f_{7/2}$ line. The additional Bi state is associated with a layer of metallic Bi, as well as the partial $\text{Eu}^{2+} \leftrightarrow \text{Eu}^{3+}$ transition. Tilting the sample does not significantly change the ratio of metallic Bi to Bi bound with Te in the Bi_2Te_3 compound. From this we conclude that the intermixing depth at the bottom interface is about 4 nm. The influence of europium on the electronic structure of tellurium is minor. Finally, when compared to a pure Bi_2Te_3 film, no significant changes were observed in the electronic structure of Bi or Te forming the top 2 nm thick Bi_2Te_3 top layer. The cap layer, therefore, seems to be unaffected by the underlying Eu layer. It is worth noting that intermixing between the Bi_2Te_3 and Eu layers occurs preferably when the Bi_2Te_3 under-layer is monocrystalline (compare Fig. 2(c1) and 2(c2) with Fig 1g and e).

TOF-SIMS depth profiles have been presented in Fig. 2d. Due to the weak signal of Te and Bi ions in TOF-SIMS measurements, the distribution of Cs_2Te^+ and CsBi^+ ions is presented. The signal-boosting Cs came from a Cs source which was used as a sputtering gun. The TOF-SIMS depth profiles indicate that Eu diffused into the Bi_2Te_3 bottom-layer (Fig 2d for Eu^+), which was accompanied by a change in the distribution of Bi. In other words, some of the bismuth ions were displaced from their original position in the layer stack (see Fig. 2d for CsBi^+). This data confirms the reaction observed in XPS measurements.

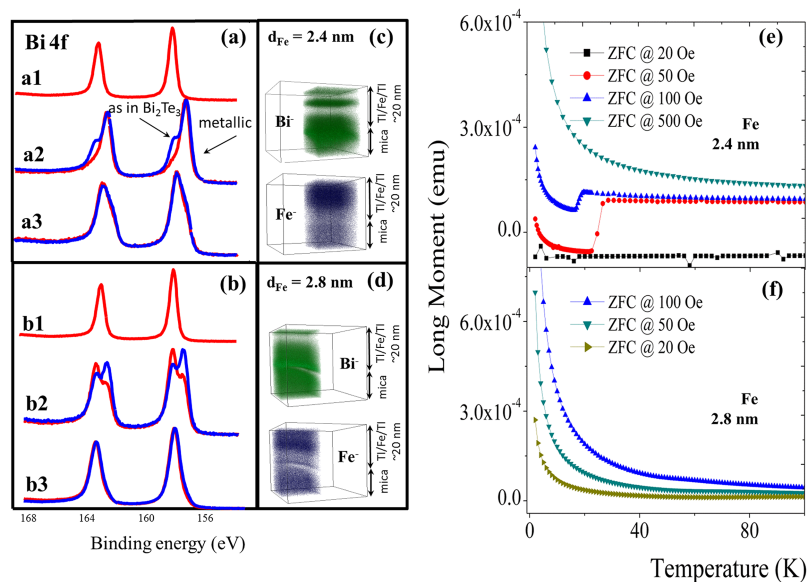


FIG. 3. The XPS photoemission spectra of (a) $\text{Bi}4f$ – obtained (a1) for 15 nm thick Bi_2Te_3 bottom layer, (a2) after deposition of 2.4 nm thick Fe layer, (a3) after deposition of 2 nm thick Bi_2Te_3 top layer. XPS of (b) $\text{Bi}4f$ – obtained (b1) for 15 nm thick Bi_2Te_3 bottom layer, (b2) after deposition of 2.8 nm thick Fe layer, (b3) after deposition of 2 nm thick Bi_2Te_3 top layer. Blue lines correspond to angle dependent XPS measurements. 3D TOF-SIMS depth profiles of (c) heterostructure with 2.4 nm thick Fe layer, (d) 2.8 nm Fe. The $M(T)$ curves obtained in zero-field-cooled experiment at several different fields for (e) heterostructure with 2.4 nm thick Fe, (f) 2.8 nm thick Fe.

For the heterostructures with Fe inter-mixing at room temperature was observed through chemical shifts of the Bi4f photoemission line indicating strong changes in the electronic structure of Bi. We relate intermixing to the reaction between Fe and Te, the reaction leads to formation of, most probably, a thin TeFe layer. The reaction leads to separation of metallic Bi. In case of heterostructure where thickness of Fe, $d_{\text{Fe}}=2.4$ nm, this is accompanied by the separation of a metallic Bi layer (see Fig.3(a2), 3(a3), 3c). The effect of segregation of metallic Bi layer are not seen in the heterostructure with a slightly different Fe layer thickness, $d_{\text{Fe}}=2.8$ nm (see Fig 3d), probably metallic Bi is distributed in FeTe+Bi₂Te₃ matrix. Angle dependent XPS measurements (see blue lines in Fig. 3a and 3b) as well as TOF-SIMS investigations (Fig.3c and 3d) allowed us to conclude that both the geometrical alignment of the layers, as well as chemical instability at both interfaces occurred in the heterostructures. Surprisingly those factors are different for two structures with slightly different Fe content. The observed at layer/mica interface curved region (see Fig. 3d) in distribution maps of Bi-and Fe-is due to different charging of heterostructure and mica.

The magnetic properties of the heterostructures containing Fe strongly depend on the processes taking place at Bi₂Te₃-Fe interfaces and the deposition conditions. More precisely, a slight difference in the thickness of the deposited Fe caused enormous changes of the magnetic properties of the system. In case of our studies, for a certain thicknesses of Fe, $d_{\text{Fe}}=2.4$ nm, a transition to a diamagnetic state was observed below (relatively high) temperatures reaching 35 K with an applied parallel to the film surface magnetic field of 100 Oe (see Fig. 3e). The M(H) curves showed a narrow (40 Oe) hysteresis loop at 2 K with the exchange bias effect. These characteristics were not observed, however, in the sample with $d_{\text{Fe}}=2.8$ nm (see Fig. 3f). This data seems to exclude the presence of superconductivity in the sample; we are probably dealing with unusual transitions between different magnetic states. An interesting question, which will be investigated in future studies, is related to possible superconductivity in the FeTe layer formed when $d_{\text{Fe}}=2.4$ nm.

IV. CONCLUSIONS

The determination of the nature and properties of novel heterostructures based on topological insulators can be used to help develop new classes of devices and technologies for future applications. The studies of two model junctions were performed in terms of chemical stability at the TI - M interfaces. From the XPS studies we showed that even at room temperature, the deposition of Fe and Eu films on well-defined monocrystalline bismuth telluride leads to chemical instability and the formation of new phases at the interfaces, such as FeTe and metallic Bi. Facts like this must be taken into account when planning and engineering future devices based on TI. In our study, we also found that the macroscopic magnetic properties of the heterostructures are very sensitive to the thickness of the Fe layer. The influence of the metallic ferromagnetic films should be studied thoroughly after taking the chemical reactions taking place at the interfaces into account. Our results indicate that both the geometry and chemical stability of such junctions have a critical influence on the magnetic properties of TI-M-TI heterostructures. *Ex-situ* characterization, for example via 3D depth profiling using a TOF-SIMS spectrometer, can help verify structural and compositional agreement between nominal/assumed vs. fabricated junctions.

¹ M. Z. Hasan and C. L. Kane, *Reviews of Modern Physics* **82**, 3045 (2010).

² X. L. Qi and S. C. Zhang, *Reviews of Modern Physics* **83**, 1057 (2011).

³ M. Eschbach *et al.*, *Nature Communications* **6**, 8816 (2015).

⁴ M. Q. He, J. Y. Shen, A. P. Petrović, Q. L. He, H. C. Liu, Y. Zheng, C. H. Wong, Q. H. Chen, J. N. Wang, K. T. Law, I. K. Sou, and R. Lortz, *Scientific Reports* **6**, 32508 (2016).

⁵ A. A. Baker, A. I. Figueroa, L. J. Collins-McIntyre, G. van der Laan, and T. Hesjedal, *Scientific Reports* **5**, 7907 (2015).

⁶ A. A. Baker, A. I. Figueroa, G. van der Laan, and T. Hesjedal, *Results in Physics* **6**, 293 (2016).

⁷ M. Jamali, J. S. Lee, J. S. Jeong, F. Mahfouzi, Y. Lv, Z. Zhao, B. K. Nikolić, K. A. Mkhoyan, N. Samarth, and J. P. Wang, *Nano Letters* **15**(10), 7126 (2015).

⁸ H. Zhang, C. X. Liu, X. L. Qi, X. Dai, Z. Fang, and S. C. Zhang, *Nature Physics* **5**(9), 438 (2010).

⁹ D. Hsieh, Y. Xia, D. Qian, L. Wray, F. Meier, J. H. Dil, J. Osterwalder, L. Patthey, A. V. Fedorov, H. Lin, A. Bansil, D. Grauer, Y. S. Hor, R. J. Cava, and M. Z. Hasan, *Physical Review Letters* **103**, 146401 (2009).

¹⁰ Y. L. Chen *et al.*, *Science* **325**, 178 (2009).

- ¹¹ U. Gradmann, H. Elmers, and M. Przybylski, *Journal de Physique Colloques* **49**(C8), 1665 (1988).
- ¹² A. R. Miedema, *Journal of the Less Common Metals* **46**, 167 (1976).
- ¹³ R. Rapacz, K. Balin, A. Nowak, and J. Szade, *Journal of Crystal Growth* **401**, 567 (2014).
- ¹⁴ R. Rapacz, K. Balin, M. Wojtyniak, and J. Szade, *Nanoscale* **7**(38), 16034 (2015).
- ¹⁵ J. Szade and M. Neumann, *Journal of Physics: Condensed Matter* **11**(19), 3887 (1999).